Laboratory Work No. 14.
Statistics of Particle Detection

This laboratory work explores statistical patterns in experimental measurements in nuclear and particle physics. Using a particle detector, we estimate the characteristics of stationary radiation fluxes and evaluate the accuracy of these estimations.

Contents

1. Introduction

The aim of this laboratory work is to study the statistical principles that underlie experimental measurements in nuclear and particle physics. We will analyze measurements of the natural background radiation level and the activity of an unknown radiation source.

The main sources of natural background radiation are nuclear radioactive decay and cosmic rays. When cosmic rays interact with the Earth's atmosphere, they generate fluxes of elementary particles, including hadrons and leptons. Thus, our area of interest includes both processes characteristic of atomic nuclei and those involving particles that constitute matter.

Nuclear and particle physics typically does not study objects as large as atoms. However, in this work we will inevitably encounter processes that also occur on the atomic scale. Therefore, we will briefly discuss some key concepts of atomic physics.

1.1. The Atom

An atom is the smallest unit of matter that retains the chemical properties of an element. As you may recall from chemistry, the typical radius of an atom is of the order of 10^{-10} m. It is important to understand that this does not refer to a well-defined geometric size since, according to quantum mechanics, atoms do not have exact geometric shapes (this is related to Heisenberg's uncertainty principle, which is not discussed in this guide but will be addressed in the nuclear and particle physics course).

We assume that the atom consists of a positively charged nucleus (with a size of the order of 10^{-15} to 10^{-14} m) which contains almost all of the atom's mass, and a surrounding cloud of point-like, negatively charged electrons. These electrons compensate for the positive charge of the nucleus, making the atom electrically neutral.

Electrons are bound to the nucleus by the Coulomb force. The energy required to remove an electron from the atom varies in the range 4 to 24 eV. For example, in a hydrogen atom, it is equal to 13.6 eV. The process of removing an electron from an atom is called ionization.

The energy scales associated with atomic processes are much lower than those common for nuclear physics and, even more so, for particle physics. In general, the smaller is the object, the higher is the energy required to study it. This reflects a principle we all know since childhood: to understand what's inside something, you have to hit it hard enough to break it. In physics, this translates into a direct link between the energy of the probing particle and the resolution it provides. The same principle applies to energy scales that characterize different levels of the microscopic world (see [1, 2], section *"de Broglie Wavelength"* for more details).

Therefore, in most cases, atomic effects can be neglected in nuclear and particle physics. Conversely, when a particle interacts with matter and its energy is not sufficiently high, ionization becomes the main observable process.

1.2. The Nucleus

An atomic nucleus carries a positive electric charge, as it consists of positively charged protons and electrically neutral neutrons, collectively referred to as nucleons. As mentioned earlier, nuclei occupy only a very small fraction of the atoms' volume, with a characteristic size of the order of 10^{-15} to 10^{-14}

meters, or 1–10 femtometers (fm). Like atoms, nuclei are not solid "balls", but rather distributions of fields.

Unlike atoms, which are governed entirely by the electromagnetic interaction, nuclei cannot be explained by electromagnetism alone. From the point of view of electromagnetic interaction, protons should repel each other, and neutrons should not interact at all. Yet, protons and neutrons are bound together inside nuclei by *the strong nuclear force.* Because this force has a very short range of about 1 femtometer, it also determines the small size of nuclei. (If the strong interaction had a long range, like electromagnetic or gravitational forces, you would definitely notice its effects in the macroscopic world: for example, your attraction to this manual would be so strong that you might never be able to put it down.)

To date, more than 3,500 different nuclei have been discovered, but only about 300 of them are stable. Nuclear stability is not an inherent property — it simply means that the nucleus has no energetically favorable way to transform into another isotope. If such a possibility exists, the nucleus will tend to decay into a more energetically favorable configuration. This property is called *radioactivity* — the spontaneous emission of particles from unstable atomic nuclei as they decay into other nuclei or lower energy states of the same isotope.

Let us now consider the N–Z diagram of atomic nuclei (see Fig. 1 - a full-scale version is available at [3]). This chart shows all known isotopes discovered to date. The horizontal axis represents the number of neutrons, and the vertical axis shows the number of protons. Stable nuclei are shown in black.

For light nuclei, *the valley of stability* (the location of stable nuclei) lies along the line $N = Z$, reflecting the tendency of these nuclei toward symmetry between the number of protons and neutrons. However, for medium and heavy nuclei, the valley curves downward, toward an excess of neutrons. This is because the nuclear radius becomes sufficiently large, while the attractive strong force only acts at short distances. Each nucleon (proton or neutron) attracts only its immediate neighbors through the short-range strong

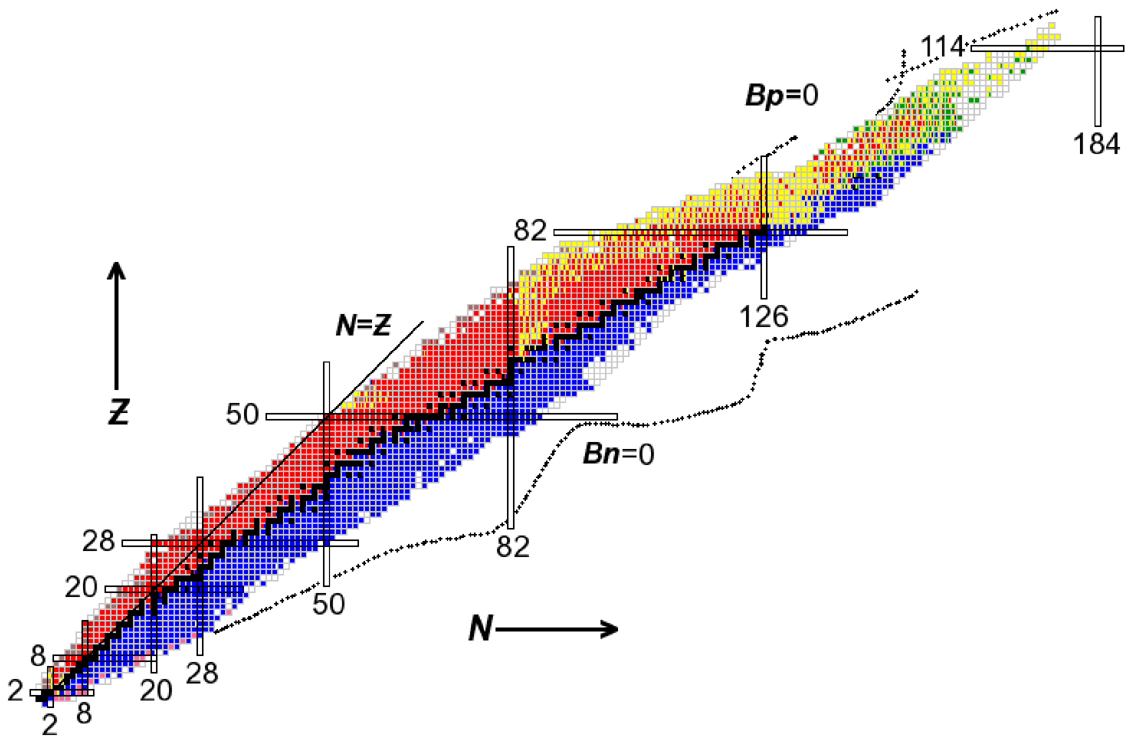

Figure 1. N–Z diagram of atomic nuclei

interaction, whereas protons repel all other protons via the long-range electromagnetic force. To balance this repulsion, a greater number of neutral neutrons is required.

The remaining nuclei are radioactive. Since the most energetically favorable configuration of nucleons in a nucleus corresponds to a higher binding of nucleons with each other and a lower nuclear mass, nuclei tend, in their transitions, toward the valley of stability (hence its name). In addition to the energetic benefit of transitions, decays are constrained by a significant number of conservation laws, leaving only a few possible decay channels for nuclei: α radioactivity, β radioactivity, γ transitions and spontaneous fission. Each color on the N–Z diagram of atomic nuclei corresponds to its own type of radioactivity.

Nuclei located below the valley of stability (blue color) have an excess of neutrons relative to protons (compared to the most favorable ratio characteristic of the valley of stability). Moreover, the further the nucleus is from the valley of stability, the higher the neutron excess. To approach the valley of stability, neutron-rich nuclei need to reduce this excess. One might think that the simplest way to achieve this is to emit neutrons. However, nuclei are strongly bound structures, and a large amount of energy is required to remove a nucleon even when sufficiently far from the valley of stability; therefore, nuclei cannot spontaneously emit neutrons.

If nuclei cannot emit neutrons, the only remaining option is to convert a neutron into a proton inside the nucleus. However, to satisfy charge conservation, something negatively charged must be created along with the proton. The lightest negatively charged particle is the electron. The next by mass hierarchy, the muon (which we will discuss in the next section) has a mass about 200 times greater than that of the electron, and there is not enough energy for its creation.

In this form, the decay reads $n \to p+e^-$, or for a nucleus with mass number (total number of nucleons) A and proton number Z: ${}^A_Z\mathrm{X} \to {}_{Z+1}^{A}\mathrm{Y} + e^-$, and this is how β^- decay was viewed until 1930. Studying the dependence of electron energy in beta decay (also known as its *spectrum*), one finds that electrons do not always have the same energy, as one would expect from the conservation laws of energy and momentum in the decay of a single body into two; rather, their energy distribution is continuous (see Fig. 2).

In 1930, Wolfgang Pauli set forth a hypothesis of a weakly interacting particle that is created during β decay and carries away an arbitrary part of the decay energy. Later, the existence of the neutrino and its antiparticle — the antineutrino — was confirmed experimentally. In β^- decay, an antineutrino is emitted:

$$n \to p + e^- + \tilde{\nu}_e,$$

$${}^A_Z\mathrm{X} \to {}_{Z+1}^{A}\mathrm{Y} + e^- + \tilde{\nu}_e.$$

Neutrinos and antineutrinos do not participate in either strong or electromagnetic interactions. We will not consider gravitational interaction here and further — it is negligible due to the extremely small masses involved. We can detect neutrinos because they participate in the remaining of the four fundamental interactions — the weak interaction, which is suppressed in probability

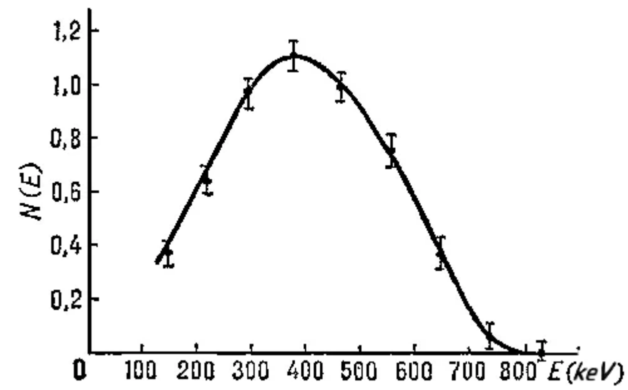

Figure 2. Energy spectrum of electrons in beta decay of the neutron. The horizontal axis shows energy, the vertical axis shows the number of registered particles.

compared to the others. However, this also leads to enormous experimental difficulties in detecting neutrinos: due to their low probability of interacting with matter, very large detector volumes are required (for example, modern neutrino telescopes such as IceCube, KM3NeT, Baikal-GVD, with size of the order of one cubic kilometer). The probability of detecting neutrinos and antineutrinos with a Geiger counter in our experiment is extremely low, so we will not dwell further on the properties of this particle.

For nuclei with a proton excess (red nuclei on Fig. 1), everything works similary, and we observe β^+ radioactive nuclei. In the process of β^+ decay, a proton inside the nucleus turns into a neutron, decreasing the nuclear charge without changing the total number of nucleons. Thus, the decay proceeds as follows:

$$p \to n + e^+ + \nu_e,$$

$${}^A_Z\mathrm{X} \to {}_{Z-1}^{\;\;\;A}\mathrm{Y} + e^+ + \nu_e.$$

It should be emphasized that β^+ decay is possible only for a proton bound in a nucleus, unlike β^- decay, which is possible even for a free neutron.

However, nuclei have another option to convert a proton into a neutron: they can capture an electron from an atomic orbital. There is a non-zero probability that an atomic electron will be inside the nucleus for a short time. The nucleus captures the electron, typically from the nearest atomic orbital, so that one of the protons in the nucleus absorbs the electron and turns into a neutron and a neutrino:

$$e^- + p \to n + \nu_e,$$

$$e^- + {}^A_Z\mathrm{X} \to {}_{Z-1}^{\;\;A}\mathrm{Y} + \nu_e.$$

Electron capture (ε-capture) is always energetically more favorable than β^+-decay, since the nucleon captures an existing electron instead of spending additional energy to produce one among the final particles. On the other hand, at nuclear energy scales, electron shells are effectively invisible, and the probability of capture is low. Thus, the competition between β^+ decay and electron capture leads to different outcomes depending on the nucleus. The regions of β^+ decay and electron capture are combined and are indicated in red.

In the region of heavy nuclei, not only does the position of the valley of stability shift due to the increasing role of Coulomb interaction relative to the strong force, but nuclei as a whole become less tightly bound. As a result, it becomes energetically favorable for them to reduce their mass number. As we discussed earlier, for most nuclei, the emission of individual protons or neutrons is unfavorable. However, there is now the possibility to emit a strongly bound cluster of nucleons. The record-holder among light nuclei in this respect is ${}^4_2\mathrm{He}$ — the most abundant isotope in the Universe after hydrogen.

Therefore, for $Z > 83$, α-decay becomes a characteristic mode of radioactive transformation — the decay of an atomic nucleus accompanied by the emission of an α-particle (isotope ${}^4_2\mathrm{He}$):

$$X(A, Z) \to Y(A-4, Z-2) + \alpha.$$

For even heavier nuclei, the channel of spontaneous fission — that is, the splitting of a nucleus into two fragments of comparable mass — becomes relevant (shown in green on the N–Z diagram). The mechanism of this process is very similar to α-decay: the nucleus also separates into two smaller nuclei.

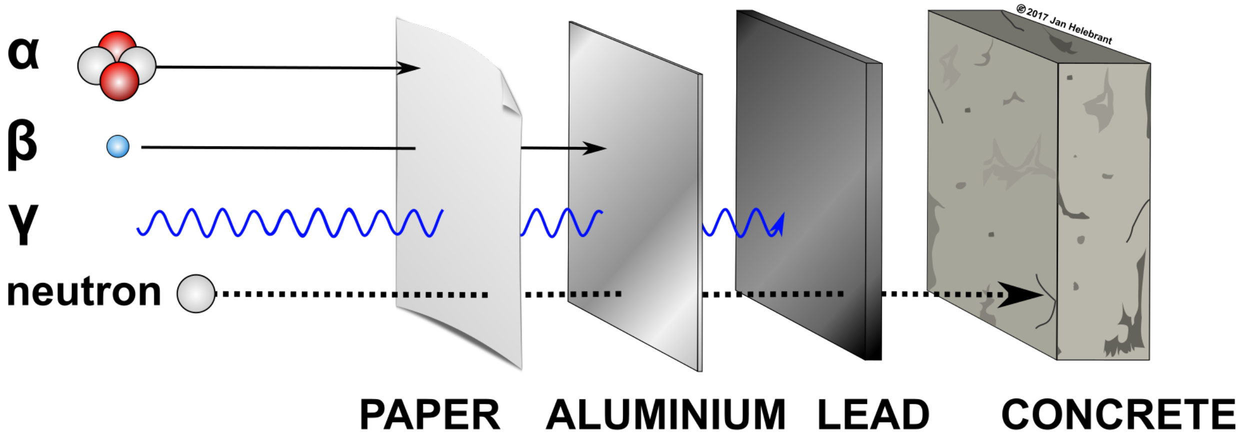

Figure 3. Penetration ability of different types of radiation: α, β, γ, and neutron.

Both processes are governed by the strong interaction (nucleons are bound by the strong force and separate without changing in number).

The penetration power of α radiation, however, is very low (and even lower for fission fragments). A simple sheet of office paper is enough to stop α particles (see Fig. 3). The Geiger counter used in this experiment is not designed to detect α-particles (although sometimes a Geiger counter is equipped with a thin mica window for this purpose). Therefore, we will leave the detailed discussion of the two processes until they become relevant in other tasks of this practical course.

Radioactive decays produce nuclei not only in their *ground states* but also in *excited* states (having the same composition but possessing higher stored energy). An excited nucleus cannot be stable, as it always has a lower-energy state available, and so it may undergo subsequent α or β decays, or it may return to its ground state via γ transitions.

A γ transition is the transition of an excited nucleus to its ground state (or to a less excited state), accompanied by the emission of a γ quantum.

In the N-Z diagram, γ transitions are not assigned a separate color, since they are not an intrinsic property of nuclei determined solely by their nucleon configuration: any nucleus can be excited by providing it with energy. Nevertheless, virtually all types of radioactivity are accompanied by secondary γ radiation.

1.3. Particles

As the characteristic energies increase, we gain access to studying objects of smaller scales. We eventually stop observing nuclear processes and begin to resolve the internal structure of the nucleons themselves. The point-like constituents of nucleons are called *quarks*. Protons consist of three quarks, two of which are the so-called up quarks (often simply denoted as u) and one is the down quark (d), while neutrons are made up of two d quarks and one u quark. All the diversity of matter around us and in the Universe can be reduced to the existence of a small number of constituents, the dynamics of which are governed by the four fundamental interactions already mentioned above: strong, weak, electromagnetic and gravitational.

In addition to u and d quarks, there exist strange (s), charm (c), top (t), and bottom (b) quarks, along with their antiparticles — antiquarks $\bar{u}$, $\bar{d}$, $\bar{c}$, $\bar{s}$, $\bar{t}$, $\bar{b}$. From the quark composition of protons and neutrons, it is simple to deduce that u and d quarks carry fractional charges:

$$\begin{cases} 2q_u + q_d = q_p = 1e, \\ 2q_d + q_u = q_n = 0, \end{cases}$$

where q_u, q_d, q_p, and q_n are the electric charges of u and d quarks, protons, and neutrons, respectively, and $e \approx 1.6 \cdot 10^{-19}$ C is the elementary charge. This relation holds for other quark types as well (see Table 1).

Quark	Quark mass	Quark charge
u (up)	2.16 ± 0.07 MeV	$+\frac{2}{3}e$
d (down)	4.70 ± 0.07 MeV	$-\frac{1}{3}e$
c (charm)	1.2730 ± 0.004 GeV	$+\frac{2}{3}e$
s (strange)	93.5 ± 0.8 MeV	$-\frac{1}{3}e$
t (top)	172.56 ± 0.31 GeV	$+\frac{2}{3}e$
b (bottom)	4.183 ± 0.007 GeV	$-\frac{1}{3}e$

Table 1. Properties of quarks.

The fact that quarks have fractional charges does not contradict the statement that e is the smallest charge observed in nature. Quarks do not exist in a free state — this phenomenon is known as *confinement*. We observe particles composed of quarks, generally called *hadrons*: *baryons* — three-quark states; *mesons* — quark–antiquark pairs; and *antibaryons* — composed of three antiquarks (see Fig. 4).

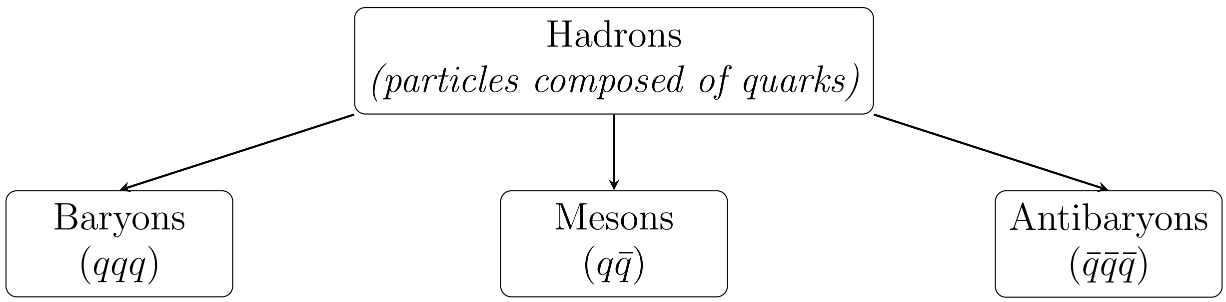

Figure 4. Classification of hadrons.

In this classification, the proton and neutron are baryons, while an example of a meson is the pion (π-meson). Charged pions have the following quark compositions: $\pi^+(u\bar{d})$, $\pi^-(d\bar{u})$. The presence of quark structure determines the particles' ability to participate in processes governed by strong interaction.

We have already encountered protons and neutrons when discussing atomic nuclei. Both are hadrons, which means they interact via the strong force — and this is precisely what allows them to form strongly bound structures which are atomic nuclei.

Not all free particles have quark structure. For example, electrons are considered to be point-like in modern physics. They belong to the second major class of particles — the *leptons*. Having no quark structure, leptons do not participate in the strong interaction. Their participation in the electromagnetic interaction is determined solely by the presence of an electric charge (unlike hadrons, whose quark structure guarantees such charges).

There are 6 leptons (+ 6 antiparticles): the electron (e^-), its heavier cousin the muon (μ^-), and the heaviest of them all — the tau lepton (τ^-), along with their three neutral partners — the neutrinos ν_e, ν_μ, ν_τ.

(At this point, the attentive — and hopefully still conscious — reader should better understand why we could not realistically expect to detect neutrinos effectively in our earlier discussion of β-decay).

Lepton	Lepton mass	Lepton charge
e^-	0.511 MeV[a]	$-1e$
ν_e	$< 4 \cdot 10^{-7}$ MeV[b]	0
μ^-	105.66 MeV[c]	$-1e$
ν_μ	< 0.19 MeV	0
τ^-	1776.93 ± 0.09 MeV	$-1e$
ν_τ	< 18 MeV	0

Table 2. Properties of leptons.

6 quarks and 6 leptons, along with 6 antiquarks and 6 antileptons, are sufficient to describe all known visible matter. We must also mention the particles associated with the fundamental interactions: in quantum theory, interactions are described not through classical fields but via the continuous exchange of mediator particles. The carrier of the strong interaction is the gluon (g), of the electromagnetic interaction — the photon (γ), and of the weak interaction — the W^+-boson, W^--boson, and Z^0-boson. The hypothetical carrier of the gravitational interaction — the graviton — is predicted by certain theories but has not yet been experimentally detected. Finally, we have the Higgs boson (H), responsible for giving mass to some particles.

The properties of these particles — collectively described by the *Standard Model* — will be studied in detail in the nuclear and particle physics course. In our case, we will only encounter some of them, as we are dealing with the largest accelerator in the Universe — cosmic space. The vast cosmic electromagnetic fields can accelerate particles to enormous energies, and when they interact with the Earth's atmosphere, they produce cascades of diverse particles (pions, muons, strange mesons such as kaons).

Before reaching the Earth's atmosphere, cosmic rays consist of accelerated charged particles, primarily hydrogen nuclei — protons (about 95% of all particles) — as well as heavier nuclei, up to iron and nickel. Protons interact efficiently with the atmosphere (since they participate in all fundamental

[a] $0.51099895000 \pm 0.00000000015$ MeV

[b] Only an upper limit is known, set by experimental uncertainty.

[c] $105.6583755 \pm 0.0000023$ MeV

interactions) and produce pions. Charged pions are short-lived particles (lifetime $\sim 10^{-10}$ s) and predominantly decay via:

$$\pi^- \to \mu^- + \tilde{\nu}_\mu; \quad \pi^+ \to \mu^+ + \nu_\mu.$$

The muon is a lepton, and due to its different interaction mechanism with the atmosphere, it has a high probability of reaching the Earth's surface. As a result, at sea level, cosmic radiation consists almost entirely of muons and neutrons.

Nuclear reactions induced by cosmic rays in the atmosphere (and partly in the lithosphere) also produce radioactive nuclei — cosmogenic radionuclides. The main isotopes of this type are ^{3}H, ^{7}Be, ^{14}C, and ^{22}Na. Despite their low concentrations in the environment, they decay relatively quickly and therefore make a noticeable contribution to the natural background radiation.

2. Statistical Regularities of Experiments in Nuclear and Particle Physics

In quantum physics, which describes nuclear physics and particle physics, the classical property of determinism is absent, i.e., **all processes and interactions are fundamentally probabilistic in nature.** This means that even an ideal experiment measuring a quantity with a macroscopic value (for example, the neutron lifetime $\tau_n \approx 900$ s) can yield practically any result. Thus, the result of an experiment in nuclear and particle physics is a random variable in nature, and methods of mathematical statistics must be applied to extract data from the experimental results.

From the statistical point of view, an experimental measurement of a physical quantity in the most general case can be described as follows. Within a given physical model, the state of a physical system is characterized by a set of physical quantities that have specific, well-defined values (*true values*), which are, however, unknown to an external observer. The goal of the experiment is to determine the true values of these quantities with the required accuracy. The experiment consists of some action performed on the system under study, the result of which is a set of *measured values* of one or more observable quantities (not necessarily those physical quantities that are of interest to measure, as they may not be directly observable). Due to various measurement errors, these measured values are random variables. At the stage of data processing, the measured values are used to obtain *estimates* of the desired physical quantities.

2.1. Parameters of Random Variable Distributions

The main characteristic of a random variable is the *distribution function* $F(x)$, which, by definition, for a random variable X is equal to the probability that $X \leqslant x$, i.e.,

$$F_X(x) = P(X \leqslant x). \tag{1}$$

In each state of the system, the distribution functions of the measured quantities are strictly defined and depend on the true values of the system parameters:

$$F_X(x) = F_X(x|\vartheta_1, \vartheta_2, \dots, \vartheta_n) \equiv F_X(x|\boldsymbol{\vartheta}), \tag{2}$$

where ϑ_i are the parameters of the physical system, and $\boldsymbol{\vartheta}$ is the vector composed of ϑ_i values. In general, there may be several quantities X_j measured in one experiment (for example, length, time, and temperature measured simultaneously), and in that case, the same parameter vector $\boldsymbol{\vartheta}$ defines several distribution functions for the measured quantities X_j. The measured quantities X_j can also be written as a vector $\mathbf{X} = \{X_1, X_2, \dots, X_m\}$, which can then be described as a random vector with a *multivariate distribution function*:

$$F_{\mathbf{X}}(\mathbf{x}|\boldsymbol{\vartheta}) = \begin{pmatrix} F_{X_1}(x_1|\boldsymbol{\vartheta}) \\ F_{X_2}(x_2|\boldsymbol{\vartheta}) \\ \vdots \\ F_{X_m}(x_m|\boldsymbol{\vartheta}) \end{pmatrix} = \begin{pmatrix} P(X_1 \leqslant x_1|\boldsymbol{\vartheta}) \\ P(X_2 \leqslant x_2|\boldsymbol{\vartheta}) \\ \vdots \\ P(X_m \leqslant x_m|\boldsymbol{\vartheta}) \end{pmatrix}. \tag{3}$$

As a result of the experiment, a value of the vector $\mathbf{X}$ is measured, i.e., m

measured physical quantities depending on n parameters. The same experiment can be repeated several times, resulting in a set of measured values of the random vector $\mathbf{X}$: $\mathbf{X}_1, \mathbf{X}_2, \ldots, \mathbf{X}_N = \{\mathbf{X}_i\}$ (in this case, the index refers not to the components X_j but to the repetition number of the experiment). This sequence is called a *sample* of the random vector $\mathbf{X}$, and ultimately, the goal of the experiment can be formulated as obtaining an estimate of the physical parameters $\boldsymbol{\vartheta}$ as some function τ of the measured sample $\{\mathbf{X}_i\}$:

$$\boldsymbol{\vartheta}^* = \tau(\{\mathbf{X}_i\}), \tag{4}$$

where the superscript "*" denotes the estimate of the true value.

The description above corresponds to the general case of an experiment in which the values of m variables depending on n parameters are measured. In this work, we will consider the simplest one-dimensional case, for which $m = n = 1$. In this case, the measurement and parameter vectors $\mathbf{X}$ and $\boldsymbol{\vartheta}$ reduce to scalars X and ϑ.

2.2. Mathematical Expectation and Variance

The estimate $\boldsymbol{\vartheta}^*$, being a function of random variables, is itself a random variable and therefore has its own distribution function, as well as standard characteristics of random variables such as *mathematical expectation* and *variance.*

To define these properties, it is necessary to introduce the concept of discrete and continuous random variables. A random variable is called *discrete* if it takes values from a set whose elements can be enumerated by natural numbers, i.e., its possible values belong to a countable set. An example of a discrete random variable is a quantity whose value is an integer (for example, a number on a roulette wheel or the side of a tossed coin).

A *continuous* random variable takes values from a continuous set. A random real number is an example of a continuous random variable.

A more visual description of random variables, compared to the distribution function, is provided by the *probability distribution* for discrete integer values and the *probability density function* for continuous variables. The probability distribution of a discrete variable is the function $P(k)$ equal to the probability that the discrete random variable takes the value k.

The probability density function of a continuous random variable X is a function $p(x)$ such that the probability of X falling within the interval $(x, x+dx]$ is $P = p(x)dx$.

The *mathematical expectation* of a discrete random variable K is

$$\mathbf{E}[K] = \sum_i k_i P(k_i), \tag{5}$$

where the index i runs over all possible values $K = k_i$.

The mathematical expectation of a continuous random variable X with a probability density function $p(x)$ is

$$\mathbf{E}[X] = \int\limits_{-\infty}^{\infty} xp(x)\, dx. \tag{6}$$

The term “mathematical expectation” is often used interchangeably with “mean value”. In mathematical statistics, they are practically synonyms, but we will use the concept of the mathematical expectation, as it explicitly indicates the random nature of the quantity, whereas the mean value is a more general term used in other areas of physics and mathematics.

In accordance with the properties of the integral, the mathematical expectation is a linear function of random variables:

$$\mathbf{E}[\alpha X + \beta Y] = \alpha \mathbf{E}[X] + \beta \mathbf{E}[Y], \tag{7}$$

where X and Y are random variables, and α and β are constants.

The *variance* of a random variable X is defined as

$$\mathbf{D}[X] = \mathbf{E}[(X - \mathbf{E}[X])^2]. \tag{8}$$

Variance measures the uncertainty or spread of a random variable around its mean. For the same purpose, the *standard (or root-mean-square) deviation* is defined as

$$\sigma = \sqrt{\mathbf{D}[X]}. \tag{9}$$

The variance of the sum of random variables equals the sum of their variances:

$$\mathbf{D}\left[\sum_{i=1}^{K} X_i\right] = \mathbf{D}[X_1] + \mathbf{D}[X_2] + \cdots + \mathbf{D}[X_K], \tag{10}$$

and the variance of a random variable multiplied by a constant factor is

$$\mathbf{D}[\alpha X] = \alpha^2 \mathbf{D}[X]. \tag{11}$$

2.3. Estimates

As mentioned above, an estimation of a parameter of a random variable distribution (or a function of these parameters) is any method of determining its value from a sample obtained through measurement. Since the input data of the estimation process are random, the estimate itself is a random variable and can therefore be characterized by its distribution function, mathematical expectation, and variance.

The *bias* of an estimate ϑ^* of some quantity ϑ is defined as

$$b = \mathbf{E}[\vartheta^*] - \vartheta, \tag{12}$$

i.e., the difference between the expected value of the estimate and the true value of the estimated quantity. If the bias is $b = 0$, the estimate is called *unbiased*. Obviously, if the bias is unknown, an unbiased estimate is preferred.

The variance of the estimate $\mathbf{D}[\vartheta^*]$ characterizes its accuracy, along with the *mean squared error* M:

$$M = \mathbf{E}[(\vartheta^* - \vartheta)^2] = \mathbf{D}[\vartheta^*] + b^2. \tag{13}$$

There may be infinitely many ways to estimate the same quantity, but in practice, one seeks an estimate with minimal bias and variance. An estimate with minimal mean squared error is called *efficient*.

2.4. Histogram and Empirical Distribution Function

After performing a series of experiments and obtaining a sample $\{x_1, x_2, \ldots, x_N\}$ of a random variable X, one can construct an *empirical distribution function*, i.e., a step function $\hat{F}(x)$ such that

$$\hat{F}(x) = \frac{\mathbb{N}(x_i \leqslant x)}{N}, \tag{14}$$

where $\hat{F}(x)$ at each point equals the ratio of the number of sample elements less than or equal to x to the total number of elements.

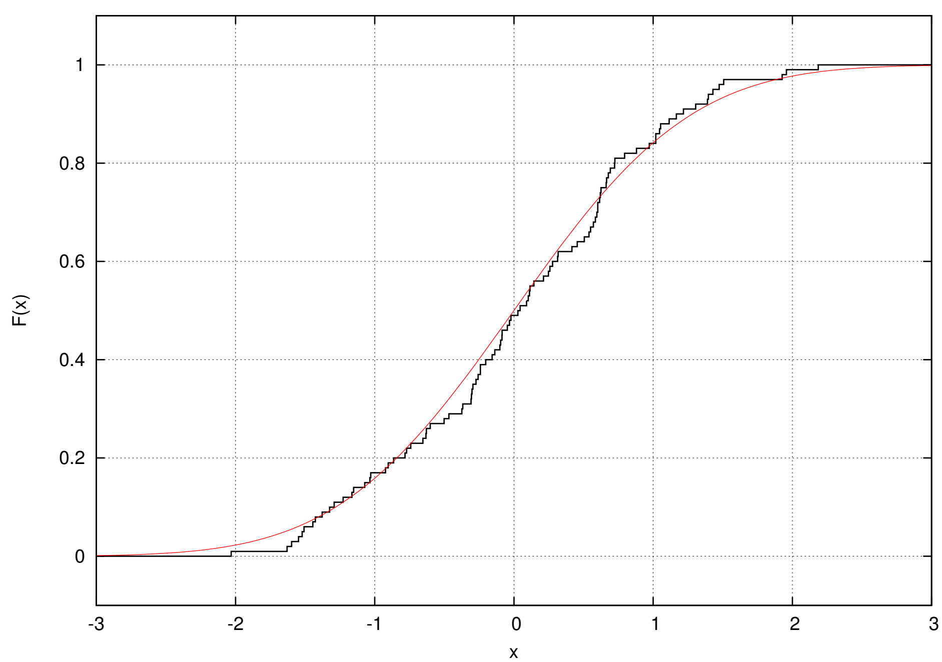

Figure 5. Empirical distribution function of a sample of 100 normally distributed random numbers.

Example. Fig. 5 shows the empirical distribution function of a sample of $N = 100$ normally distributed random numbers, along with the distribution function corresponding to these numbers. As the sample size N increases, the empirical distribution function becomes smoother and approaches the "true" distribution function.

For a visual representation of measured data, histograms are constructed. To build a histogram for a measured sample $\{x_i\}$:

1) choose the range $[x_{\min}, x_{\max})$ for the histogram;

2) select the number of histogram bins K, dividing the range $[x_{\min}, x_{\max}]$ into K intervals. The width of each bin is $\Delta x = (x_{\max} - x_{\min})/K$, and the boundaries of the k-th bin correspond to $[\Delta x\,(k-1), \Delta x\,k)$;

3) count the number n_k of sample elements $\{x_i\}$ falling within each bin;

4) plot the histogram as a bar graph, where the height of each bar is $h_k = n_k$. Alternatively, a *frequency distribution* can be plotted with $h_k = n_k/(N\Delta x)$, so each bar represents the relative frequency rather than the absolute count.

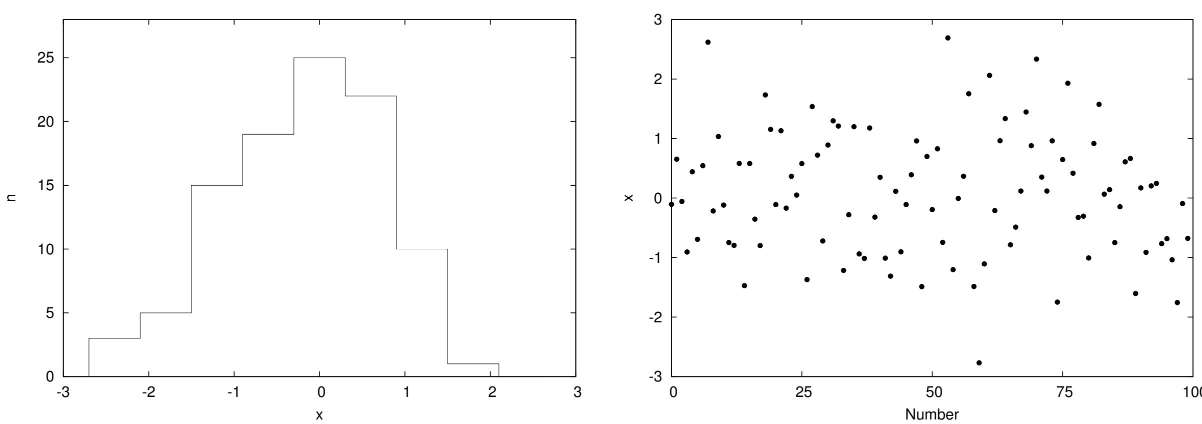

Figure 6. Right panel: histogram for the same random numbers as in Fig. 5. Left panel: original points versus measurement number.

2.5. Kolmogorov Goodness-of-Fit Test

Comparing the empirical distribution functions of two random variables allows one to determine whether their distributions coincide. For this purpose, the Kolmogorov-Smirnov test is used. According to this test, the hypothesis of identical distributions (homogeneity) of two samples $\{x_i\}$, $i = 1, 2, \ldots, N$, and $\{x'_j\}$, $j = 1, 2, \ldots, N'$, is tested as follows:

1) compute the empirical distribution functions $\hat{F}(x)$ and $\hat{F}'(x)$;

2) find the supremum $D = \sup_x |\hat{F}(x) - \hat{F}'(x)|$, i.e., the maximum difference between the two empirical distributions;

3) calculate the statistic $t = \sqrt{\frac{NN'}{N+N'}}\, D$;

4) if t exceeds K_α, the homogeneity hypothesis is rejected at the confidence level $1 - \alpha$; otherwise, the hypothesis is accepted (see K_α values in the table).

Table 3. Confidence levels of the Kolmogorov-Smirnov test

$1 - \alpha$	K_α
0.5	0.82757
0.6	0.89476
0.7	0.97306
0.8	1.0727
0.9	1.2238
0.95	1.3581
0.99	1.6276
0.999	1.9495
0.9999	2.2253

2.6. Estimation of the Mean, Standard Deviation, and Standard Error

The main numerical quantity determined in Task №14 is the intensity of natural background radiation events, i.e., the number of background particles detected per unit time. To find it, one must compute the average number of particles recorded during the measurement time. The mean value of a random variable is its mathematical expectation, and the best way to find this value is the *efficient estimate of the mathematical expectation.*

Note that there is no general formula for the efficient estimate for arbitrary distributions. However, for the Poisson and normal distributions encountered in this work, the efficient estimate of the mean based on a measured sample $\{x_i\}$ is given by

$$\mu^* = \frac{1}{N}\sum_{i=1}^{N} x_i, \tag{15}$$

where N is the sample size, i.e., the efficient estimate coincides with the *arithmetic mean* of the sample.

In addition to the mean estimate μ^*, its accuracy should be known, expressed by the standard deviation. The standard deviation of the mean estimate is called the *standard error* and is computed as

$$\sigma_\mu = \sqrt{\frac{\mathbf{D}[X]}{N}} = \frac{\sigma}{\sqrt{N}}. \tag{16}$$

One commonly used method to estimate variance from a measured sample $\{x_i\}$ is

$$\mathbf{D}^*[X] = \frac{1}{N-1}\sum_{i=1}^{N}(\mu^* - x_i)^2, \tag{17}$$

where μ^* is computed as above. Then, the estimate of the standard deviation is:[d]

$$\sigma^* = \sqrt{\frac{1}{N-1}\sum_{i=1}^{N}(\mu^* - x_i)^2}. \tag{18}$$

Thus, the commonly used formula for the standard error of the mean is:

$$\sigma^*_\mu = \frac{\sigma^*}{\sqrt{N}} = \sqrt{\frac{\sum_{i=1}^{N}(\mu^* - x_i)^2}{N(N-1)}}. \tag{19}$$

[d]This is an example of a non-efficient estimate: σ^* is biased relative to the true standard deviation. The factor $(N-1)^{-1}$ reduces bias for small sample sizes N.

3. Properties of Probability Distributions

3.1. Binomial Distribution

Consider a sequence of elementary experiments, each of which results in one of two outcomes, "1" and "2" (for example, "heads" or "tails" in a coin toss). Let the probability of one outcome be p, then the probability of the other outcome is $q = 1 - p$. Suppose the experiment is repeated N times, and consider a random variable k – the number of experiments resulting in outcome "1". This sequence of experiments is called a *Bernoulli scheme.* We want to find the law governing k, i.e., the probability distribution $P(k)$.

The probability of k occurrences of outcome "1" is proportional to p^k. Additionally, the remaining $N - k$ experiments result in outcome "2", which is accounted for by the factor $(1-p)^{N-k}$. Finally, the last factor accounts for the fact that $p^k(1-p)^{N-k}$ describes the probability of only one specific sequence of outcomes in the Bernoulli trials. To account for all possible combinations of k successes out of N, the *binomial coefficient* is used:

$$C_k^N = \frac{N!}{k!(N-k)!}. \tag{20}$$

Thus, the probability of obtaining k outcomes "1" in a series of N experiments is

$$P(k) = C_k^N p^k (1-p)^{N-k}. \tag{21}$$

This distribution is called the *binomial distribution.* Its mean and variance are

$$\mathbf{E}[k] = Np, \quad \mathbf{D}[k] = Np(1-p). \tag{22}$$

3.2. Statistical Laws of Nuclear Decay

Before considering limiting cases of the binomial distribution, let us discuss general laws related to the decay of nuclei or particles. For convenience, we refer to nuclear radioactive decay, but particle decay follows the same laws.

Consider the radioactive decay of N nuclei confined in a certain volume.

The general behavior of radioactive isotopes can be estimated under the assumption that the decay probability λ is constant for each isotope (commonly called the *decay constant*). The number of nuclei at a given time t can be obtained by solving the differential equation relating the change in the number of nuclei per unit time to the total number of nuclei (see Lab Work No. 1 for details), giving:

$$N(t) = N_0 \mathrm{e}^{-\lambda t}. \tag{23}$$

This relation is usually called the *law of radioactive decay*. The *half-life* is the time required for the number of nuclei of an isotope to decrease by half. From the decay law, the half-life is related to the decay probability as:

$$T_{1/2} = \frac{\ln 2}{\lambda}. \tag{24}$$

The half-life alone does not provide complete information about the number of emitted particles, though it characterizes the properties of an isotope. The same isotope, taken in different amounts, may in one case emit enough particles to observe its radioactivity, and in another case produce only a small background signal. To describe this effect, the quantity *activity* A is introduced — the average number of nuclei decaying per unit time. It can be calculated by multiplying the decay probability by the number of nuclei at time t:

$$A(t) = \lambda N(t). \tag{25}$$

Activity is measured in curies (1 Ci = $3.7 \cdot 10^{10}$ decays/s) and becquerels (1 Bq = 1 decay/s).

3.3. Poisson Distribution

During time t, each nucleus may decay with probability

$$p = 1 - e^{-t\frac{\ln 2}{T_{1/2}}} = 1 - e^{-\lambda t}. \tag{26}$$

This corresponds to a Bernoulli scheme, and the total number of decays k follows a binomial distribution. In the case where $N \gg k$ (many nuclei, few decays in a short time), the binomial distribution can be approximated by the Poisson distribution:

$$P(k) = C_k^N p^k (1-p)^{N-k} \approx \\ \approx \frac{\mu^k e^{-\mu}}{k!}, \tag{27}$$

where $\mu = N\lambda t$.

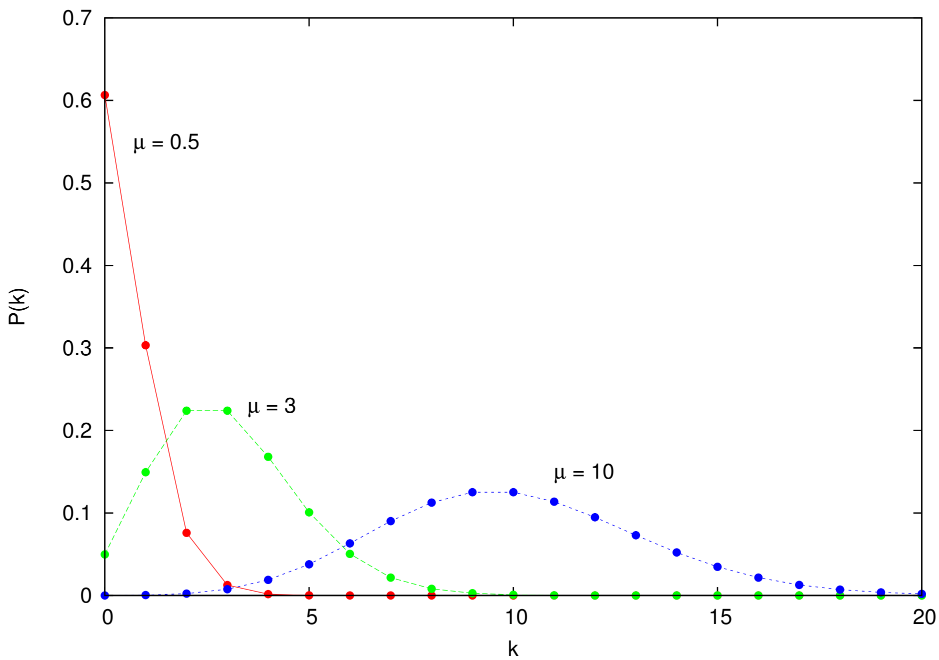

Figure 7. Poisson distribution for different values of the parameter μ.

The mean and variance of a random variable distributed according to the Poisson law are

$$\mathbf{E}[k] = \mu, \quad \mathbf{D}[k] = \mu, \quad \sigma = \sqrt{\mathbf{D}[k]} = \sqrt{\mu}. \tag{28}$$

3.4. Normal Distribution

As μ increases, the Poisson distribution becomes more symmetric, and its discreteness becomes negligible. For sufficiently large μ, the Poisson distribution can be approximated by the normal distribution:

$$P(k) \approx N[\mu, \sqrt{\mu}](k), \tag{29}$$

where the probability density function of the normal distribution is

$$N[\mu, \sigma](x) = \frac{1}{\sqrt{2\pi}\sigma} \exp\left(- \frac{(x-\mu)^2}{2\sigma^2} \right). \tag{30}$$

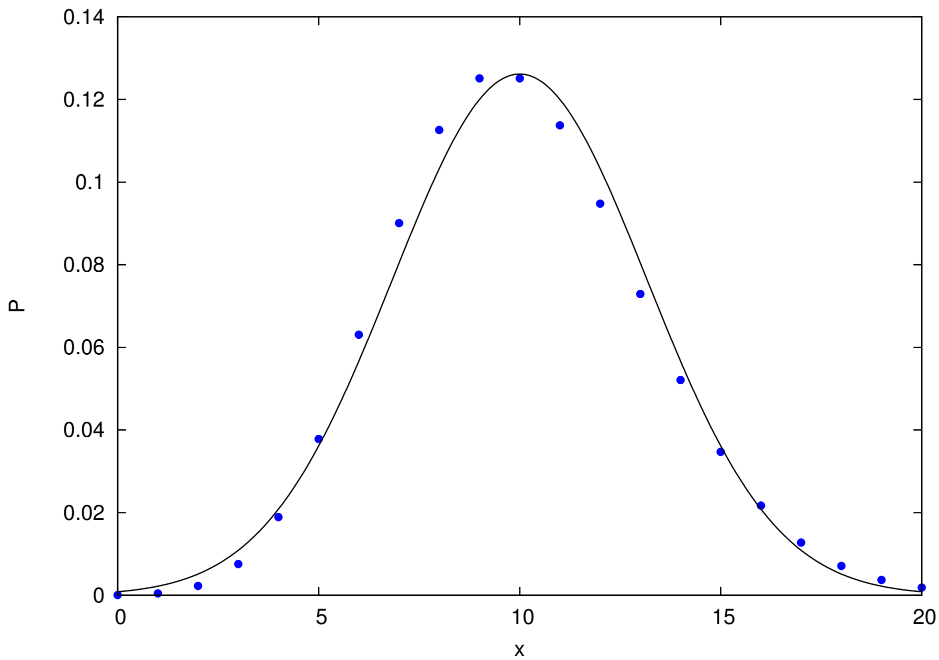

Figure 8. Comparison of the normal distribution $N[\mu, \sigma](x)$ and the Poisson distribution for $\mu = 10$.

For the normal distribution, the mean and variance are:

$$\mathbf{E}[x] = \mu, \quad \mathbf{D}[x] = \sigma^2. \tag{31}$$

4. Experimental Setup

The schematic of the experimental setup used for this work is shown in Fig. 9. The setup includes:

1) a Geiger–Müller counter designed to detect ionizing particles;

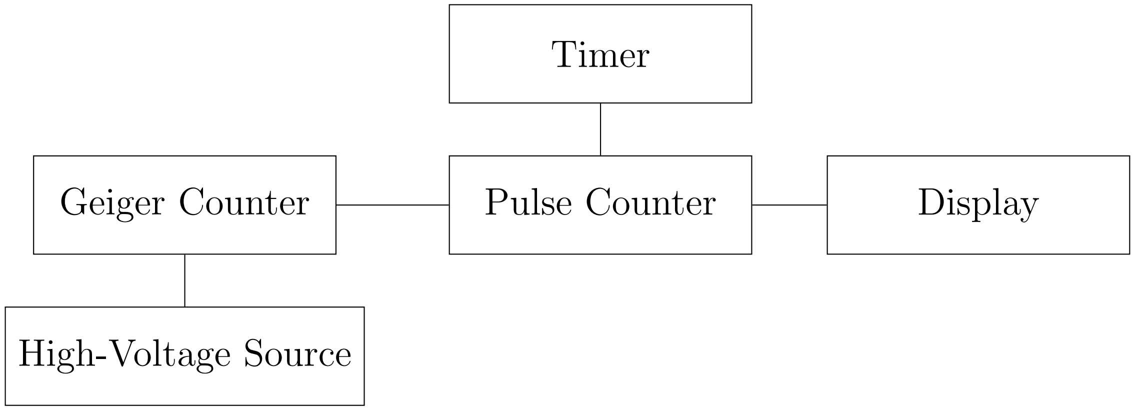

Figure 9. Diagram of the experimental setup.

2) a high-voltage converter that serves as the power supply for the Geiger–Müller counter;

3) a digital pulse counter for registering voltage pulses at the output of the Geiger–Müller counter;

4) a digital timer that automatically stops the pulse counter after a preset time;

5) an electronic display with a keyboard for outputting results and controlling the device.

All elements of the experimental setup are mounted inside a plastic housing. The Geiger counter is positioned diagonally along the top cover.

Warning! The setup includes a high-voltage source. Handle the instrument very carefully. It is strictly forbidden to disassemble or damage the housing of the device.

4.1. Operating Principle of the Geiger–Müller Counter

The Geiger counter belongs to a broad group of gas-filled detectors, which, due to their high sensitivity to various types of radiation, relative simplicity, and low cost, are widely used for radiation detection. Such a detector consists of a gas-filled volume with two electrodes. A constant voltage is applied to

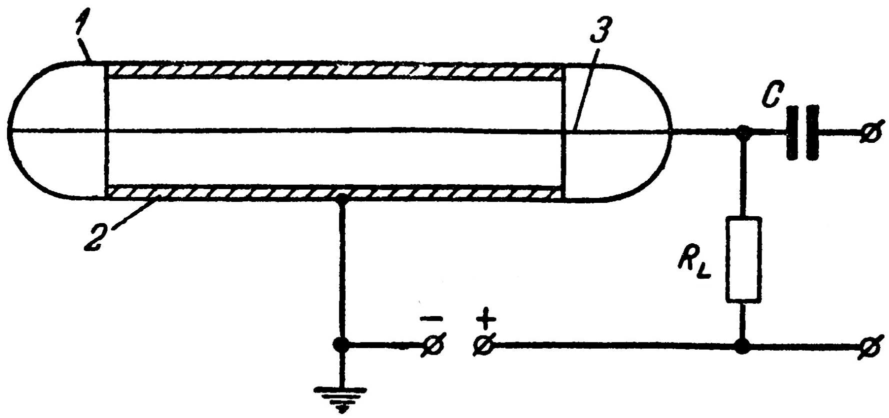

Figure 10. Gas-discharge counter, its construction, and typical wiring. 1 — glass tube; 2 — metal cylinder (cathode); 3 — wire (anode).

the electrodes. The operating voltage depends on the gas pressure, which may vary over a wide range for different detector operating modes.

Particle detection occurs as follows. A fast particle entering the counter ionizes the gas. The electrons and heavy positive and negative ions produced by the ionizing particle move in the electric field and undergo multiple collisions (elastic and inelastic) with gas molecules. The average drift velocity of electrons and ions is proportional to the electric field strength and inversely proportional to the gas pressure. The resulting current is mainly due to electrons, as their mobility is three orders of magnitude higher than that of heavy ions. The voltage pulse across the resistor R_{L} is amplified and sent to the recording apparatus.

Fig. 11 shows the dependence of the output pulse amplitude on the applied voltage (assuming that the time constant $\tau = R_{\mathrm{L}}C$ is much larger than the charge collection time in the detector). Curves α and β correspond to different initial ionizations, higher for curve α. These curves are called the counter's voltage-current characteristics. Each curve can be divided into characteristic regions.

At low voltages two competing processes occur: charge collection at the electrodes and recombination of ions in the gas. Increasing the voltage increases ion drift velocity, reducing the probability of recombination.

In region I, nearly all charges produced in the detector are collected by the electrodes. This region is called the ionization chamber region. Detectors

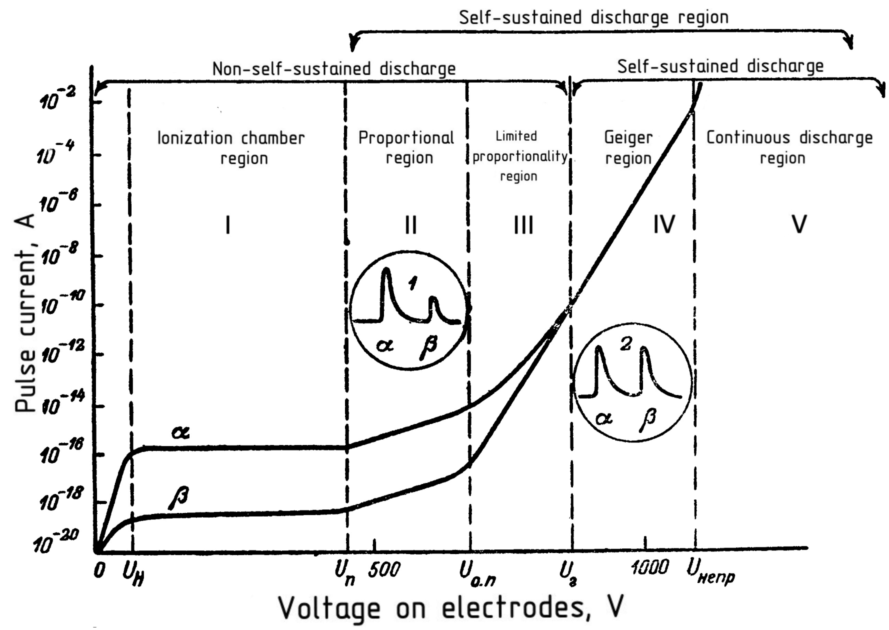

Figure 11. Voltage-current characteristic of a typical gas-discharge counter in different operating modes. The shape of pulses from α- and β-decays is schematically shown.

operating in this region are called *ionization chambers.*

At higher voltages, electrons produced by primary ionization are accelerated enough to ionize neutral gas atoms upon collision, producing secondary ions. This is called *gas amplification.* Initially, the pulse amplitude increases proportionally to primary ionization — the proportional region. In region II, so-called *proportional counters* operate.

The proportional region is followed by the limited proportionality region III.

Finally, in region IV, gas amplification becomes so large that the collected charge no longer depends on primary ionization. This is the Geiger region. The discharge remains triggered, i.e., it starts only after an ionizing particle passes through.

Further voltage increase leads to continuous self-sustained discharge (region V), which is unsuitable for particle detection.

In the Geiger counter, gas amplification is so high that secondary ionization reaches saturation. Near the threshold of this region, conditions for avalanche ionization occur only near the wire (e.g., in cylindrical counters at $V = 1000$ V, the field E at the cathode is hundreds of V/cm, and near the wire — $20000 \div 40000$ V/cm). Increasing voltage enlarges the avalanche region, and secondary ionization rapidly increases, forming an electron avalanche.

Thus, the counter undergoes a breakdown; the discharge covers the entire gas volume. Large voltage pulses appear on the anode, independent of primary ionization. Formation of even a single ion pair triggers a full discharge. In the Geiger region, the gas amplification factor reaches 10^{10}, and pulse amplitude amounts to several volts or tens of volts.

The detector geometry is chosen based on its operating conditions. A cylindrical counter consists of a metallic or metal-coated glass tube and a thin wire along the cylinder axis. The wire serves as the anode, the tube — as the cathode. End-window counters have an input window at the end. Counters are usually used for short-range particles, so the window is made of thin film.

Filling gases are usually special mixtures (e.g., Ar + HCl + HBr) with quenching additives to improve the detector's response time.

Geiger counters are highly sensitive to ionizing radiation. However, they cannot differentiate radiation types or energies, thus they measuring intensity only. An important feature is the counting plateau: the number of registered pulses is nearly independent of voltage, as each ionizing particle triggers an avalanche. Further voltage increase leads to spontaneous discharge.

The operating voltage is chosen in the middle of the plateau. Threshold voltage, plateau position, and length are specific to each counter and should be determined experimentally, usually ranging from several hundred to a thousand volts.

Geiger counters are simple, reliable, and efficient. Their sensitivity depends on particle penetration: only particles entering the active volume are detected, so wall or window thickness should not exceed particle range. Any particle producing at least one ion pair will almost certainly be detected.

To restore sensitivity after each registration, the gas must clear of heavy ions. During this *dead time*, the counter cannot register new particles. Geiger counters have relatively long dead times: 10^{-4}–10^{-3} s, and resolution does not exceed a few thousand counts per second.

Counters are also insensitive to γ-rays. Detection occurs only via secondary charged particles, produced in the counter walls, made of high-Z material. Detection efficiency is usually only 1–2%.

If a material with a high neutron cross-section is placed in the detector, neutron capture reactions produce detectable particles. Slow neutrons are often detected using boron trifluoride counters, where α-particles are produced in $^{10}\mathrm{B}(\mathrm{n}, \alpha)$ reactions. Fast neutrons are detected using hydrogen-rich detectors, where recoil protons produce the discharge.

5. Experimental Procedure

In each exercise, the pulse counter measures the number of background radiation particles detected over a fixed time. The results for each exercise are recorded in a table:

Exercise №____

Measurement duration $\Delta t =$ ____,   number of measurements $N =$ ____.

Measurement #	Number of pulses
1	
2	
...	
100	

5.1. Data Collection

5.1.1. Exercise №1. Background measurement.

1) Choose a measurement duration Δt between 30–40 s.

2) Set Δt on the timer according to the instrument manual.

3) Perform $N = 100$ measurements of the number of particles detected in time Δt.

4) Record the results in the table.

5.1.2. Exercise №2. Measurement of an unknown source.

1) Place the unknown source on the top of the detector.

2) Use the same measurement duration Δt as in Exercise 1.

3) Perform $N = 100$ measurements of the number of particles detected in time Δt and record them in a table.

Warning! Do not move the source on the detector during the entire series of measurements.

6. Data Analysis

The data from both exercises are analyzed together.

1) For each series, calculate the mean count μ^* using formula (15) and the standard error of the mean (19).

   The standard error can also be estimated differently: the Poisson variance can be approximated from the mean, giving the standard error via formula (16). Comparing both methods allows checking if the observed distribution follows the Poisson law.

   Also calculate the average *counting rate* and its error using

$$I = \frac{\mu}{\Delta t}. \tag{32}$$

2) Represent measurement results from both exercises as frequency histograms. For comparison, plot both histograms on the same page, with identical X-axis limits and bin width Δx. Original frequency values are first recorded in a notebook.

3) On each histogram, also plot: points — theoretical Poisson probabilities with parameter $\mu = \mu^*$, solid curve — normal distribution with $\mu = \mu^*$, $\sigma = \sqrt{\mu^*}$.

4) Construct empirical distribution functions for both exercises and check sample homogeneity using the Kolmogorov criterion. Record results in a table like Table 4.

   Then find the maximum absolute difference between empirical distributions and calculate statistic t. If t exceeds K_α for confidence level $1-\alpha$,

x	$\mathbb{N}(x_i \leqslant x)$		$\hat{F}(x)$		$\lvert\hat{F}(x) - \hat{F}'(x)\rvert$
	Ex. 1	Ex. 2	Ex. 1	Ex. 2	
$x_{\min}$					
$x_{\min} + 1$					
$\ldots$					
$x_{\max}$					

Table 4. Empirical distribution functions. Here $x_{\min}$ and $x_{\max}$ are the minimum and maximum counts in both exercises, $\mathbb{N}(x_i \leqslant x)$ is the number of measurements with counts not exceeding x, and $\hat{F}(x)$ is the empirical distribution function from formula (14).

the homogeneity hypothesis is rejected, indicating that the distributions differ, i.e., the unknown source is radioactive.

5) If the source is radioactive, determine its counting rate using

$$I_{\text{total}} = I_{\text{background}} + I_{\text{source}}. \tag{33}$$

Knowing the source mass, ^{40}K natural abundance $\nu = 0.012\%$, half-life $T_{1/2}(^{40}\text{K}) = 1.248 \cdot 10^9$ years, and potassium content in the sample, estimate the probability of detecting β-decays from ^{40}K, considering that the detector covers 10% of the full solid angle.

6) If no radioactive isotope is present, measurements from Exercise 2 are used to refine the background counting rate.

To submit the work, provide:

1) tables of experimental measurements;
2) histograms with overlaid theoretical calculations;
3) mean counts and counting rate for each exercise;
4) comparison of standard error estimates from both methods;
5) graphs of empirical distributions and the result of the homogeneity test for the source;
6) counting rate from the source and estimated detection probability (if present) or refined background counting rate;
7) conclusions from the experiment.

References

[1] Loveland W. D., Morrissey D. J., Seaborg G. T. *Modern Nuclear Chemistry* / 2nd ed. — Hoboken, NJ: Wiley, 2006. — 1056 p.

[2] Griffiths D. J. *Introduction to Elementary Particles* / 2nd ed. — Weinheim: Wiley-VCH, 2008. — 456 p. *(For a detailed discussion of the de Broglie wavelength and its relation to physical scales, see page 6.)*

[3] Chart of Atomic Nuclei https://www.nndc.bnl.gov/nudat3/